Detailed studies of the nuclear dependence of F_2 in light nuclei.

J. Arrington (Spokesperson), D. F. Geesaman,

K. Hafidi, R. J. Holt, D. H. Potterveld, P. E. Reimer

Argonne National Laboratory, Argonne, IL

R. Ent, H. Fenker, D. Gaskell (Spokesperson), D. W. Higinbotham,

M. Jones, D. J. Mack, D. G. Meekins, G. Smith, P. Solvignon, S. A. Wood

Jefferson Laboratory, Newport News, VA

A. Daniel (Spokesperson), K. Hicks, P. King

Ohio University, Athens, OH

F. Benmokhtar

Carnegie Mellon University, Pittsburgh, PA

P. Markowitz

Florida International University, Miami, FL

M. E. Christy, C. E. Keppel, M. Kohl, L. Tang

Hampton University, Hampton, VA

G. Niculescu, I. Niculescu

James Madison University, Harrisonburg, VA

X. Jiang, A. Puckett

Los Alamos National Laboratory, Los Alamos, NM

V. Sulkosky

Massachusetts Institute of Technology, Cambridge, MA

D. Dutta

Mississippi State University, Mississippi State, MS

L. El Fassi, R. Gilman

Rutgers University, Piscataway, NJ

W. Brooks

Universidad Técnica Federico Santa María, Valparaíso, Chile

G. Huber

University of Regina, Regina, SK, Canada

S. Malace

University of South Carolina, Columbia, SC

N. Fomin

University of Tennessee, Knoxville, TN

H. Baghdasaryan, D. Day, N. Kalantarians

University of Virginia, Charlottesville, VA

F. Wesselmann

Xavier University of Louisiana, New Orleans, LA

A. Asaturyan, A. Mkrtchyan, H. Mkrtchyan, V. Tadevosyan, S. Zhamkochyan

Yerevan Physics Institute, Armenia

(Dated: December 14, 2009)

Abstract

We propose to perform inclusive electron scattering measurements from several light to medium heavy nuclei over a broad range of x $(0.1 < x < 1)$ up to $Q^2 \approx 15$ GeV^2. These data will improve on existing JLab measurements of the EMC effect by extending precise extraction of the EMC ratios to larger x values, and by making additional measurements on light nuclei $(A < 12)$ to provide better data for constraining calculations of nuclear effects in these well understood nuclei. Because results from Jefferson lab do not support the previous A-dependent or density-dependent fits to the EMC effect, including an expanded set of light nuclei will help investigate the role of the detailed nuclear structure and test the idea that the *local* nuclear environment plays an important role in the modification of quark distributions. The proposed measurements will provide precise data in the large x region where binding and Fermi motion effects are thought to dominate, providing strict constraints on the "conventional" nuclear physics that is a key component in any calculation of the EMC effect. In addition, a better understanding of the EMC effect in light nuclei will provide guidance for calculation of nuclear effects in deuterium, which is necessary to extract neutron structure function, while new measurements of the deuteron and proton structure functions at large x will provide new data for such extractions.

I. CONTRIBUTION TO THE HALL C 12 GEV UPGRADE

The co-spokespersons for this experiment plan to contribute to the implementation of the JLAB and Hall C upgrade for 12 GeV in both manpower and materials.

David Gaskell will support the SHMS construction and detector assembly and is responsible for ensuring functionality of the Hall C Møller and Compton polarimeters at 12 GeV. In addition, he will devote time to updating and maintaining the Hall C simulation package SIMC. This will entail, not only incorporating the SHMS into the existing simulation, but helping with spectrometer optics calculations.

The Medium Energy Physics group at Argonne has responsibility for the initial optics design and the optics commissioning of the SHMS, and is coordinating the trigger, data acquisition, and analysis software.

Aji Daniel is contributing to the prototyping and construction of the pre-shower calorimeter for CLAS12 in Hall B. He will also contribute to the commissioning and checkout of the SHMS in Hall C.

II. INTRODUCTION AND MOTIVATION

A. Overview

The question of the nuclear dependence of the quark structure of nuclei, as measured in deeply-inelastic scattering (DIS), has been of great interest since the European Muon Collaboration (EMC) [1] found significant deviation between the structure functions of heavy (iron) and light (deuterium) nuclei. Since then, the nuclear dependence of structure functions has been extensively studied, both experimentally and theoretically (see Refs [2–4]), and yet while there are extensive data on the x and A dependence of the EMC effect, its origin is not yet well understood.
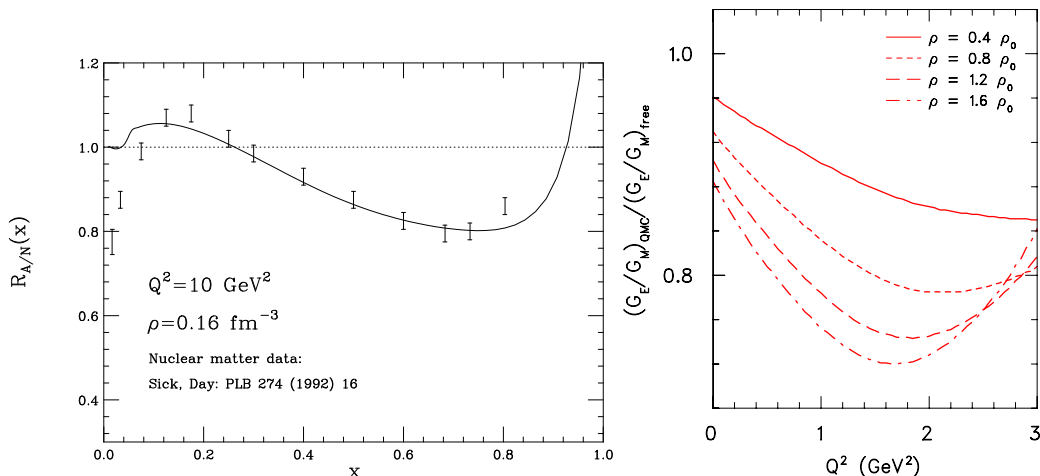

FIG. 1: Calculation of the EMC effect for Nuclear Matter (left) and modification to the in-medium proton form factors (right) from the Quark-Meson Coupling model.

Along with measurements in the DIS region, experiments have looked for more direct evidence of modification to the nucleon structure via measurements of in-medium form factors, most recently taking advantage of high precision recoil polarization measurements of G_E/G_M [5], which have become possible with the advent of high current, high polarization electron beams and high efficiency recoil polarimeters. Recent calculations [6, 7] are able to make predictions for both the structure function and form factor modification in nuclei, making these measurements very powerful in conjunction with the DIS measurements (as illustrated in figure 1). These new measurements are meant to directly connect to the in-medium form factors, and are expected to be significantly less sensitive to final state interactions or other nuclear effects than previous attempts to constrain the in-medium form factors via explicit Rosenbluth separations or inclusive measurements of quasielastic scattering (*e.g.* the Coulomb Sum Rule). However, while the final state interactions are believed to be small, it has been shown [8] that these final state interactions can have a

non-trivial effect on the results, and may be sufficient to explain the apparent signal of form factor modification in ^{4}He [5].

Other measurements have been performed or suggested that may be able to increase our understanding of the origin of the EMC effect. Recent work by Miller and Smith use a Chiral soliton model to relate the EMC effect and nucleon form factor modification [9], but also examine the EMC effect in polarized [10] and unpolarized [11] structure functions, and the nuclear dependence of Drell-Yan scattering [12]. The prediction for the polarized EMC effect shows the largest difference in the region of anti-shadowing, but the prediction is quite different from the QMC model prediction [6]. Recent works by Marco, *et al.*, also calculate the EMC effect and nuclear dependence of Drell-Yan in a common framework [13, 14] (figure 2).
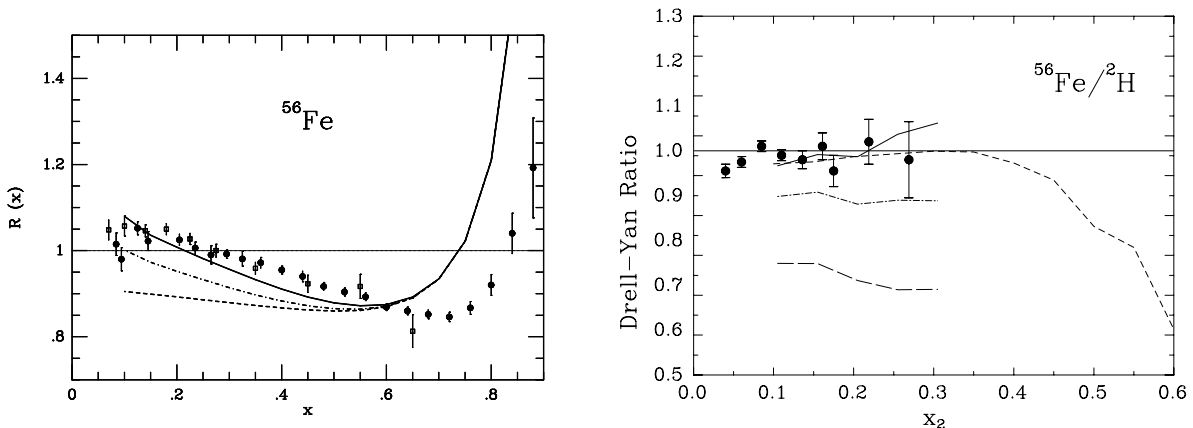

FIG. 2: Calculation of the EMC effect from Ref. [13] (left) and the Drell-Yan nuclear dependence [14] (right). For the EMC effect, The solid lines include the nucleonic and mesonic (pions and rhos) contributions, the dashed lines contain the contribution fro nucleons alone, and the dot-dashed line ratios shows the contribution from nucleons and pions. Data are from SLAC and BCDMS and NMC. The Drell-Yan ratios are from Fermilab E772 [15], and the curves correspond to nucleonic (long-dashed), nucleon and pion (dot-dashed), and full (solid) calculations.

While measurements of in-medium form factors are meant to offer a more direct test of the modification of nucleon structure in nuclei, the experimental signature is not as clean as the DIS measurements. Data on the nuclear dependence of Drell-Yan scattering is limited to lower x values, while the spin-dependent EMC ratios are technically challenging and require significant theoretical input on nucleon polarization in nuclei. On the other hand, while the measurements of the EMC effect are a clear signature of a nuclear dependence of the structure functions, the complete explanation for this modification is theoretically difficult to isolate, as smearing, binding effects, and other possible nuclear corrections may all be contributing. *Thus, it is important to continue efforts on multiple fronts; extending measurements aimed*

at directly probing in-medium form factors, examining the nuclear dependence of polarized structure functions or anti-quark distributions, and extending the measurements of the EMC effect into regions where the data can better constrain theoretical explanations of the effect.

B. SLAC and CERN measurements of nuclear structure functions

In DIS kinematics where both the four momentum transfer, Q, and the energy transfer, ν are large, the extracted structure functions are independent of Q^2 except for the well understood logarithmic QCD scaling violations. In the scaling region the structure function is interpreted as the incoherent sum of quark distribution functions. Significant differences in the inelastic structure function (per nucleon) of Fe and deuterium were observed by the European Muon Collaboration (EMC) [1] over a large range in Bjorken x.
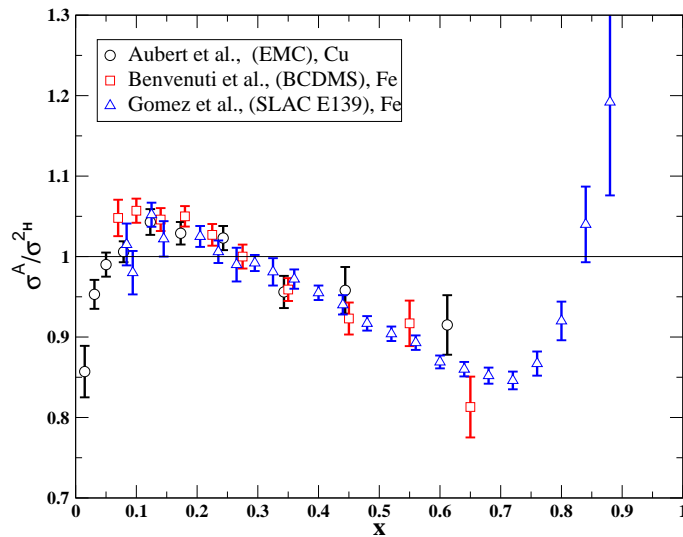

FIG. 3:   Shown are the representative cross section ratios (Fe or Cu to ^{2}H) as a function of x measured at different facilities with different beam types and energies. Data are from [16–18]

.

After the initial observation of an unexpected nuclear dependence in the structure functions of heavy nuclei, further measurements were performed at both CERN and SLAC, as shown in Fig. 3 for measurements emphasizing large x). Further measurements by the EMC collaboration, and later the New Muon Collaboration (NMC) [19, 20], significantly improved the precision and kinematic range of measurements at low x, mapping out in detail the shadowing region for a range of nuclei. The SLAC measurements, in particular experiment E139 [18] mapped out the high x region for a range of nuclei, yielding a measurement of the A dependence of the EMC effect, as shown in Figs. 4 and 5.
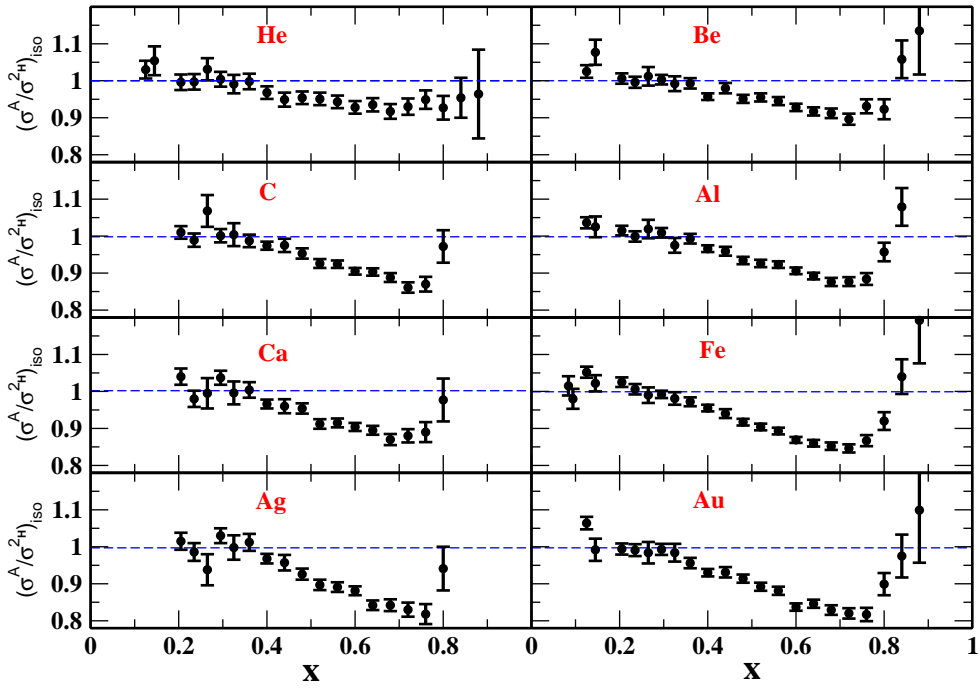
FIG. 4: Q^2 averaged iso-scalar corrected cross section ratios from SLAC E139. The errors shown are the combined statistical and point-to-point systematic errors.
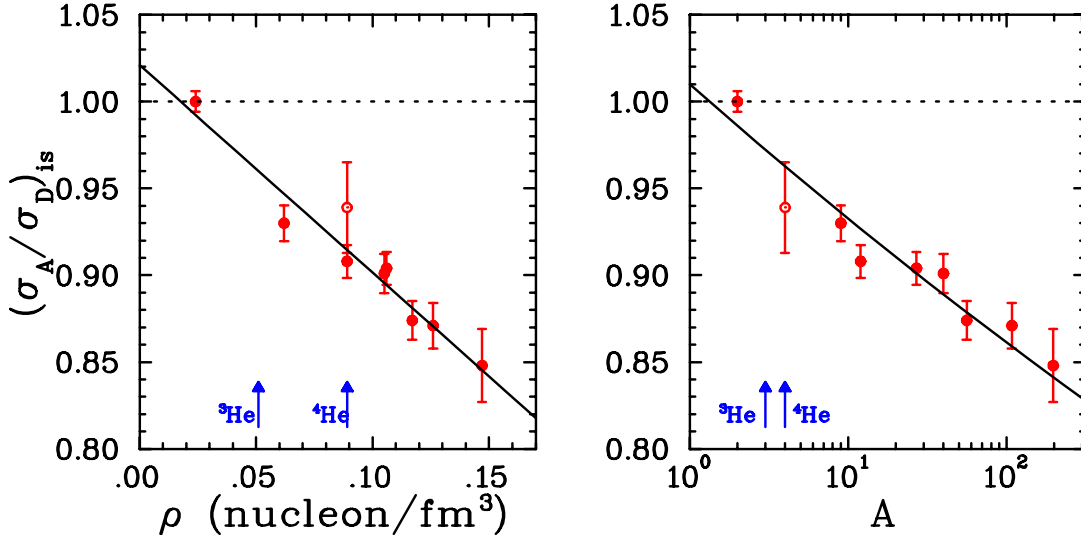

FIG. 5: SLAC fit to the EMC ratio at $x = 0.6$ as a function of A and ρ. The arrows indicates where ^{3}He and ^{4}He are located.

While several measurements were performed, there were still limitations on how well these results could be used to constrain explanations of the EMC effect. These measurements show a universal shape for the EMC ratios in the valence region, and a weak dependence on A. However, the A dependence can be well fit with either a simple A-dependent or rho-

dependent form [18], thus making it difficult to test models of the EMC effect based on the A dependence. In addition, the EMC effect at very large x values is not well measured. The constraint that the data be taken in the DIS region ($W^2 > 4$ GeV^2) forced measurements to be taken at higher Q^2, led to measurements being limited by the cross section at large x, where the pdfs fall relatively rapidly.

Because the nuclear dependence appears to have contributions from multiple effects, it has been difficult to determine exactly what causes the observed behavior. The effects of binding and Fermi motion are important at all x values, and must be understood to provide a 'baseline' expectation for effects at lower x values (as illustrated in fig. 2). These effects are the dominant contributions at large x, but the limited data at large x, coupled with the lack of precise data on light, easily calculable nuclei, has made it difficult to determine how well these 'traditional' nuclear physics effects are being included in models of the nuclear structure function.

So while the general x dependence and A dependence of the EMC effect were relatively well mapped out, they did not provide sufficiently strong constraints on the models of the EMC effect.

C.   JLab E03-103

1.   Aim of the proposal

The goal of JLab experiment E03-103 [21] was to try and address some of these limitations in previous measurements of the EMC effect. The experiment made precise measurements at large x and focused on light nuclei (^{3}He, ^{4}He, ^{9}Be, and ^{12}C), to allow for comparisons to calculations using realistic models of nuclear structure in the region where the traditional effects of binding and Fermi motion are believed to dominate. The data on ^{4}He yielded significantly higher precision than from E139 due to the use of a high density cryotarget which was not available for E139. E03-103 also provided the very first high precision measurements of the EMC effect in ^{3}He at large x values.

E03-103 was able to accumulate much better statistics at high x than E139 because of the increased luminosity at JLab, and because we took advantage of the fact that scaling in nuclei is observed at lower W^2 in nuclei then in the proton [22, 23]. This was first examined in the EMC ratios using data from 4 GeV measurements [24], which showed that the nuclear dependence at much lower W^2 values was still in good agreement with measurements in the DIS region, even down to $Q^2 \approx 3$ GeV^2 and $W^2 \approx 1.5$ GeV^2. For E03-103, the main data was taken at Q^2 values somewhat below the SLAC kinematics, but the Q^2 dependence was directly measured at several Q^2 values (kinematics shown in Fig. 9), and the EMC

ratios showed no significant Q^2 dependence for $Q^2 > 4$ GeV^2 up to $x \approx 0.85$, as shown in figure 6. Even at higher x values there was no indication of a clear Q^2 dependence, but the data were not precise enough to set tight limits on the Q^2 dependence. These data demonstrate quantitatively the ability to reliably extract the nuclear dependence at larger x than previous measurements by relaxing the typical DIS cuts on W^2, providing high precision measurements of the EMC effect in light nuclei up to $x \approx 0.85$. This data can be used to precisely evaluate models of nuclear effects in a set of light nuclei where the uncertainty due to the detailed nuclear structure is minimal.

There was a second motivation for the focus on these very light nuclei in E03-103. If the EMC effect is explained in part by modification to the quark substructure of the nucleons in a nucleus, then one possible mechanism is the interaction of quarks in nucleons that are very close together. In these cases, the overlap of the nucleons may allow for a direct exchange of quarks (and momenta) between the nucleons. We know that these short range configurations are an important contribution to nuclear structure and increase as one goes to heavier nuclei [25–28]. If these two-body interactions contribute to the nuclear dependence, then the details of the EMC effect, in particular the x dependence, may look different in few-body nuclei than in heavy nuclei, as was predicted by some of the very few calculations available for few-body nuclei at the time [29, 30]. While the results of E03-103 show that the x dependence is consistent in both very light and very heavy nuclei, the A dependence in light nuclei yielded a surprising result.

2. *Results of E03-103*

The full results for the EMC ratios for ^{3}He, ^{4}He, Be and C are available in Ref. [21] (attached as an appendix). The results for all these nuclei are consistent with the SLAC measurements, with much better precision for ^{4}He and new measurements for ^{3}He. Figure 7 shows the size of the EMC effect for these light nuclei as a function of the scaled nuclear density. To avoid contributions from the normalization uncertainty in the measurements, especially important for nuclei with a small EMC effect, we quantify the size of the EMC effect based on the slope of the EMC ratio in the linear region between $x = 0.35$ and $x = 0.7$. This is essentially equivalent to what one obtains if the data sets are normalized to $R = 1$ at $x = 0.3$, where there appears to be a universal crossover point (as has been done in some comparisons of the A-dependence). For the density in these light nuclei, the assumption of a uniform sphere density distribution, as used in the SLAC fits, is not a good approximation. We take the density distributions calculated from the *ab initio* Green's Function Monte Carlo calculations [31] to calculate the average density for each nucleus. We choose to scale down this average nuclear density by a factor of (A-1)/A, based on the idea that each nucleon is
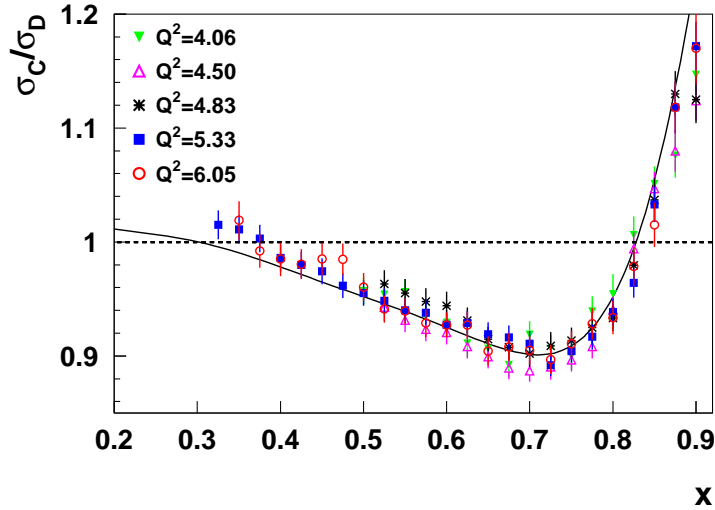
FIG. 6: Ratio of C and ^{2}H, cross sections for the five largest Q^2 settings (represented by different symbols and colors) as a function of x. The Q^2 values quoted are for $x = 0.75$. The solid curve is the SLAC ln(A) parameterizations for the EMC ratios [18].

only influenced by the other (A-1) nucleons. One could remove this factor, and while the densities would change significantly for the light nuclei, the qualitative conclusions do not change.
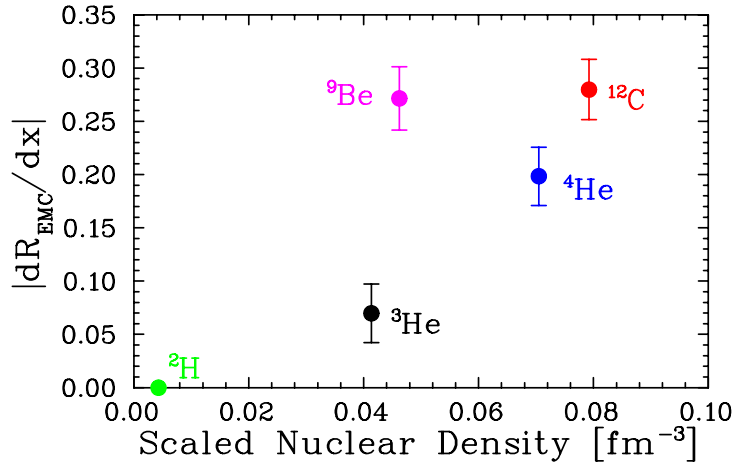

FIG. 7: The figure shows the slope of the isoscalar EMC ratios for $0.35 < x < 0.7$ as a function of scaled nuclear density (as described in the text).

Figure 7 shows an unusual behavior for the EMC effect in light nuclei. Of the four nuclei in the data set, two are very light nuclei (A=3,4), and two are somewhat heavier nuclei (A=10,12). In addition, ^{3}He and ^{9}Be have similar densities, which are significantly lower than the densities for ^{4}He and ^{12}C. If the data behaved according to the A-dependent fit of figure 5, one would expect ^{3}He and ^{4}He to be similar in magnitude and roughly a factor of two lower than ^{9}Be and ^{12}C. The density-dependent fit would predict similar values for

10

^{4}He and ^{12}C, with significantly lower effects for ^{3}He and ^{9}Be. The E03-103 results show ^{3}He has a much smaller EMC effect than either ^{4}He or ^{9}Be, suggesting that neither the mass-dependent or density-dependent parameterizations describe these light nuclei.

While neither of these simple models for the scaling of the EMC effect accurately represent the data in light nuclei, the data are consistent with the idea that the nearby nucleons are most important. The structure of ^{9}Be includes a significant component with two alpha clusters and one excess neutron. In this picture, most of the nucleons (and all of the protons) are bound in these tight clusters, and thus the local environment of the nucleons is similar to ^{4}He, even though the average density is quite low. This suggests that these clustering effects and the local environment may be important, and clearly shows that calculations of the EMC effect must take into account the detailed nuclear structure, as it is insufficient to simply scale the effects by mass, density, Fermi momentum. This further elucidates the need for precise measurements on a range of well understood nuclei, and highlights the importance of being able to perform calculations of the EMC effect and other observables (*e.g.* Nuclear dependence of Drell-Yan scattering, polarized EMC effect, and in-medium nucleon form factors) using realistic nuclear models. Such calculations are already beginning to appear, e.g. the QMC calculations of the EMC effect, proton form factors in ^{4}He, and the polarized EMC effect [6, 7, 32, 33], which includes shell-model nuclear structure for the polarized EMC effect.

In addition to extending measurements of the EMC effect to lighter nuclei and larger x values, E03-103 also focused on improving the corrections applied to the measurements. For the iso-scalar corrections, previous measurements (SLAC E139) used a correction based on the high Q^2 measurements of the free F_{2n}/F_{2p} ratio. The goal is to correct the data on the heavy target for the difference between the measured nucleus, *e.g.* 26 proton and 30 neutrons for iron, and an isoscalar nucleus with the same mass. Therefore, one should be using proton and neutron structure functions at kinematics of the experiment, as one is correcting the cross sections measured at those kinematics. In addition, because one is correcting the nuclear cross sections, one should be using the contributions of F_{2p} and F_{2n} to the nuclear structure function instead of using the free proton and neutron structure functions. This improved procedure yielded a smaller correction for ^{3}He at large x [21] than using the SLAC parameterization, and would yield a similar reduction in the effect for heavy nuclei, as ^{3}He and ^{197}Au have isoscalar corrections of opposite sign but approximately equal magnitude. However, the correction is still quite large (as seen in Fig. 8.

It was also observed that for heavy nuclei, the impact of Coulomb distortion was not negligible, even for the SLAC measurements [34]. Both the Coulomb distortion and the isoscalar correction have a strong A dependence, and therefore are important in the extrapolation to nuclear matter. For light nuclei both the ^{3}He and ^{9}Be results have significant isoscalar
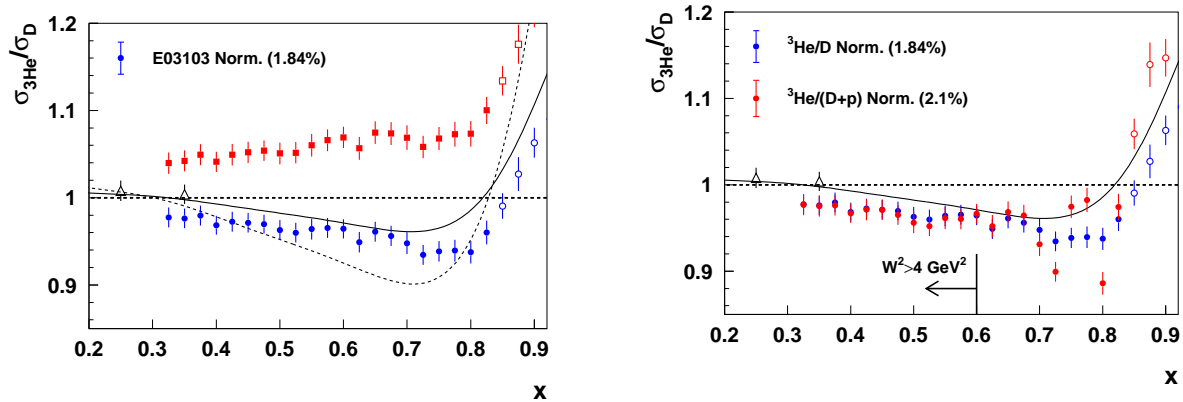
FIG. 8: The left panel shows the raw and isoscalar-corrected ^{3}He/^{2}H ratios, compared to the SLAC fit for ^{3}He and Carbon. The right panel shows the same isoscalar ^{3}He/^{2}H ratios (blue points) and the ^{3}He/(^{2}H+^{1}H) ratio (red points) extracted from E03-103 data. The black curve is the SLAC mass number dependent fit to ^{3}He.

corrections. While the corrections have been more carefully evaluated for E03-103, and it has recently been shown that the model-dependence in the neutron extraction is smaller than previous believed [35, 36], this still yields a theoretical uncertainty in these important nuclei. One way to avoid this is to take the ratio of ^{3}He to the sum of ^{2}H and ^{1}H. This allows one to compare to calculations while minimizing the impact of the uncertainty in the neutron structure function. However, for the kinematics of the 6 GeV measurement, proton resonance structure spoils the extended scaling observed in nuclei (as shown in Fig. 8), limiting the x range where the result is independent of Q^2 to $x \lesssim 0.65$.

III.   THE PROPOSED 11 GEV MEASUREMENTS

While the data from E03-103 have provided important new information on the EMC effect, there are important limitations that can be improved upon with the proposed measurements.

- The nuclei included in E03-103 were sufficient to examine the simple A-dependent and density-dependent scaling models, and show that detailed calculations including realistic nuclear structure will be important in explaining the EMC effect. *Additional light nuclei, including nuclei with significant clustering contributions, will provide further information on the detailed behavior in these well-understood nuclei.* In particular, while ^{4}He and ^{9}Be are especially well suited to separating the A-dependent and density-dependent pictures, scaling based on the *local* density, as estimated from two-body correlation functions from the GFMC calculations, yield predictions in between

12

the A and ρ dependence. *For $^{6,7}Li$, the local density picture predicts and EMC effect well below the other models.*

- For the light non-isoscalar nuclei, in particular for ^{3}He, there is a significant isoscalar correction applied to form the isoscalar EMC ratios. One can avoid the uncertainty associated with this correction, and thus better evaluate models of the EMC effect, by taking the ratio of ^{3}He to (^{2}H+^{1}H). However, the resonance structure in the proton is not washed out, and so the extended scaling observed in nuclei is not as effective, limiting the useful range for this ratio to $x \lesssim 0.65$ for E03-103 (Fig. 8). For the proposed measurements, the resonance structure shifts to larger x values and becomes a much smaller, yielding a negligible deviation from the DIS limit up to x=0.85 *Thus, the data on ^3He (and other non-isoscalar nuclei) can be precisely compared to detailed calculations, without the uncertainty associated with knowledge of the neutron structure function.* This can also be done for other light, non-isoscalar nuclei (e.g. ^{7}Li), to allow for calculations that are insensitive to knowledge of the neutron structure function.

- The higher beam energy will increase the region of precise scaling, to larger x values; going from x=0.6 to 0.8 for $W^2 > 4$ GeV^2, and up to $x = 0.92$ for $W^2 > 2$ GeV^2, where precise scaling was observed at the lower Q^2 values of E03-103. In addition, extending the measurements down to $x \approx 0.1$ will let us better compare the shape (x dependence) of the EMC effect in these nuclei. This is especially important for some of the light nuclei, where the the normalization uncertainties (*e.g.* due to absolute knowledge of the target thickness) become a limiting factor in determining the size of the EMC effect at large x. *This will provide a much better test of the A independence of the shape of the EMC effect in these light nuclei.*

- Including additional non-isoscalar targets will allow for additional tests of the EMC effect. First, there have been recent suggestions of a significant isospin-dependence for the EMC effect [33, 37]. While this would yield to a modified A dependence of the EMC effect in heavy nuclei, the neutron excess generally increases slowly with mass, and is difficult to disentangle from the global A dependence. *Measurements of ^{40}Ca and ^{48}Ca will provide a significant variation of the n/p ratio in the nucleus, while maintaining a comparison between nuclei of similar mass and density.* In addition, comparisons of nuclei which differ by just one proton or one neutron will, in principle, allow the extraction of the structure function of a single nucleon in the nucleus. This can be used to a check the isoscalar corrections applied in these nuclei, as well as providing a measurement of the nuclear effects on a single proton or neutron. For such tests, it is important to have nuclei where the nuclear structure is well understood,

e.g. $A \leq 12$, so that the effects of the binding and Fermi motion within any particular model can be reliably calculated.

- The importance of nuclear effects is not limited to heavy nuclei; understanding of nuclear effects in deuterium is an important issue since deuterium data are often used as the source of information on the neutron structure functions. Current data for the neutron structure function come from measurements of deuterium and hydrogen, using models of the nuclear effects to remove the proton contribution to the deuterium measurements [35, 36, 38, 39]. The ^{2}H and ^{1}H data taken for comparison with the ^{3}He data will provide additional high precision measurements of ^{2}H/^{1}H at high x values. Given a particular model, these data can be used to extract F_{2n}, and then the model and the neutron structure function can be tested against the measured ^{4}He/^{2}H and ^{3}He/^{2}H ratios. These data are of particular interest now, based on recent extractions of the neutron structure function (or up and down quark distributions) which suggest that the model dependence of these procedures is smaller than previously believed [35, 36].

- The precise measurement of the EMC effect in ^{6}Li and ^{7}Li will also have side benefits for polarized target measurements that use LiH or LiD targets as effective polarized proton or deuteron targets. The EMC effect modifies the dilution factor from the Li nuclei, and since the E03-103 results show that the EMC effect does not simply scale with density, a direct measurement will determine if these corrections have been appropriately applied. In addition, there have been discussions of measuring the spin-dependent EMC effect using a polarized ^{7}Li target. The comparison of the spin-dependent and spin-independent EMC ratios is important in separating out spin-dependent effects from contributions which globally rescale the quark distributions. Having high precision measurements of the unpolarized EMC effect for ^{7}Li over a large x range will be beneficial to these studies. Our measurement will be free of contamination from protons in the target, and having precise measurements over a large x range will allow for careful evaluation of calculations of the unpolarized EMC effect, to verify that the details of the nuclear structure effects are well understood before attempting to interpret additional spin-dependent effects.

IV. DETAILS OF THE PROPOSED MEASUREMENTS

A. Kinematic coverage

Figure 9 shows the proposed kinematic coverage at 11 GeV as a function x and Q^2. The data above $Q^2 = 1$ GeV^2 and at $W^2 > 4$ GeV^2 are in the conventional DIS region. It should
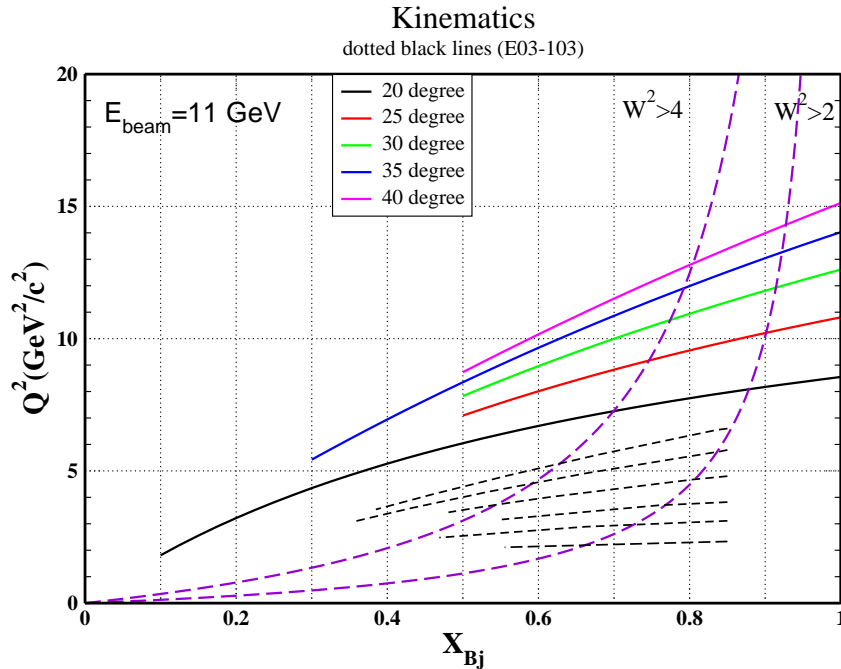
FIG. 9: Overview of the proposed kinematics. The black dotted lines are the kinematics from E03-103. Data from 20 and 35 degrees will be used for the EMC ratio extraction. Data on a small subset of targets at additional angles will be used to study the Q^2 dependence of the ratios and also to perform tests on the radiative correction procedure, charge symmetric backgrounds and rate dependent effects. The dashed lines correspond to contour of fixed invariant mass as noted in the figure.

be noted that, for E03-103, data were taken up to $x \approx 1$, but we exclude measurements beyond $x = 0.85$ because the verification of the Q^2 independence of the result becomes much less precise. Because of the high Q^2 values of the proposed experiment, the $W^2 > 2$ GeV^2 region that showed precise scaling at 6 GeV extends to $x = 0.92$. We will take additional Q^2 dependence measurements on a subset of target in the large x region to precisely define the region of scaling. These measurements will include data on the deuteron and proton structure functions, which will also provide improved measurements of the ^{2}H/^{1}H ratio at largest x, which can be used to constrain high x extractions of the neutron structure function [35, 36].

B. Experimental requirements

We propose a measurement of inclusive electron scattering from hydrogen, deuterium, ^{3}He, ^{4}He, ^{6,7}Li, ^{9}Be, ^{10,11}B, ^{12}C, ^{40,48}Ca, and ^{63}Cu. Also, data will be taken on a separate dummy aluminum target for subtraction of the target end-cap contributions. In addition,

θ (deg)	E' (GeV)	x range (for $W^2 > 2$)	Q^2 (GeV^2)	targets	estimated time (hours)
20	1.6–6.4	0.1–0.87	2.1–8.4	^{1}H,^{2}H,^{3}He,^{4}He, ^{6}Li, ^{7}Li,^{9}Be,^{12}C,^{63}Cu	24
25	3.4–5.1	0.5–0.90	7.1–10.5	^{1}H,^{2}H,^{12}C	11
30	2.7–4.2	0.5–0.91	7.8–12.3	^{1}H,^{2}H,^{12}C	31
35	1.4–3.5	0.3–0.92	5.4–13.5	^{1}H,^{2}H,^{3}He,^{4}He,^{7}Li,^{10}B, ^{11}B,^{12}C,^{40}Ca,^{48}Ca	318
40	1.7–2.8	0.5–0.93	8.7-14.6	^{1}H,^{2}H,^{3}He,^{12}C	197

TABLE I: Kinematics for the proposed measurements. All data will be taken at 11 GeV beam energy. The upper limit shown for x is for $W^2 > 2$. However, $x=1$ region also will be in the spectrometer acceptance and will be collecting data with reduced statistical precision. Both HMS and SHMS will be collecting data simultaneously.

data will be taken at high x at additional scattering angles for a subset of targets (deuterium and C) to examine the Q^2 dependence of the structure functions and EMC ratios. We will use Cu targets of different radiation lengths (2% and 6%) in order to check the corrections from external bremsstrahlung. Scattered electrons will be measured in the HMS and SHMS spectrometers, which will run independently. All data will be taken at the highest beam energy available (here 11 GeV is assumed). The HMS will be mainly used to take the low x data, while the HMS and SHMS will both take data at the larger angles, covering the large x, high Q^2 part of the measurement.

Table I lists the kinematics we propose to measure, corresponding to the kinematics shown in Fig. 9. In all cases, data will be obtained utilizing 4 cm cryotargets, an aluminum 'dummy' target and several solid targets. Most of the solid targets that will be used have been used in previous Hall C experiments (for example E03-103). One notable exception are the ^{6}Li and ^{7}Li targets. For these targets, we will require that the target be in thermal contact with the cryotarget ladder, rather than be placed on a separate solid target ladder as is commonly done in Hall C. This will allow us to run higher currents without undo heating of the lithium target material. Even so, we estimate that we will be able to run at most 15 μA on a rather thin (300 mg/cm^2) target. In the case of calcium targets, there is an already approved experiment [40] which make use of them. The run times for the ^{40}Ca, ^{48}Ca (4% radiation length) are calculated by assuming that we will be able to run at most 30 μA. The ^{11}B and ^{10}B targets will actually be made of Boron carbide (B4C) so subtraction of the contributions from carbon will be required (run times reflect the extra time needed to account for this dilution).

We will run at currents between 15 and 80 μA with 11 GeV beam energy. We will

also take hydrogen elastic data for calibration at each angle setting, as well as background measurements in regions where the charge-symmetric background may not be negligible.

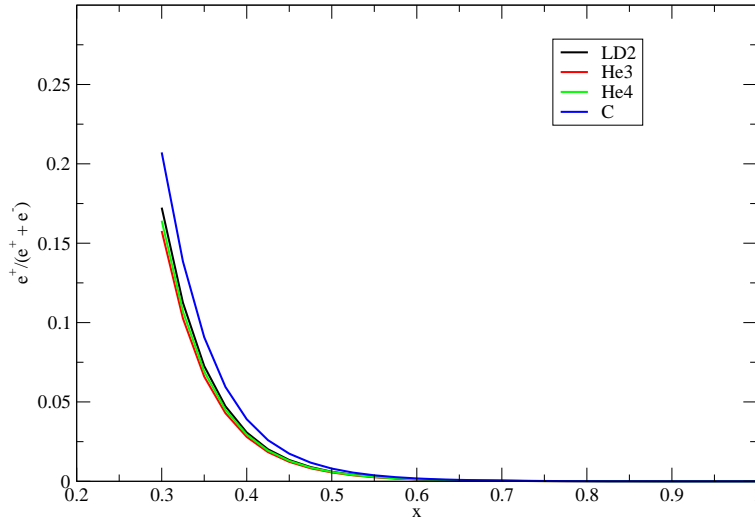## C. Estimation of backgrounds and other corrections

FIG. 10: Estimated charge symmetric background as a function of x for 35 degree data.

The background mainly consists of scattered electrons from the cryotarget cell wall, pions that survive the nominal PID cuts and mimic scattered electrons and the secondary electrons that are produced from pair production in the target after the beam electron emits a bremsstrahlung photon, producing a π^0.

E03-103 used a dummy aluminum target to directly measure the cell wall contribution to the total yield. The proposed experiment will also use a thicker dummy target to mimic the cell wall contribution, and data will be taken at the same kinematics as the cryotarget data. Dummy data will be treated in the same way as cryotarget data and the normalized dummy yield will be subtracted from cryotarget yield.

Pions are another potential source of background for the measurement. In the worst case we estimate the $\pi : e$ ratio to be on the order of 100; for most settings, the $\pi : e$ ratio is much smaller. The combination of the calorimeter and Cerenkov detectors in the HMS (SHMS) which provides a pion rejection factor of at least 10,000 (4,000) should be be adequate. Note that for the settings with the worst $\pi : e$, the HMS will be used due to its superior pion rejection.

In certain kinematic regions, there is a significant probability that the incident electron can interact with the target nuclei and produce neutral pions in the target. These pions can decay into high energy photons, which can produce an equal number of positrons and electrons. The total number of electrons detected in the spectrometer is $e^-_{detected} = e^-_{primary} + e^-_{background}$. Since an equal number of positrons and electrons are produced, the yield is charge symmetric (CSBG). This allows us to estimate the number of secondary background electrons by running the spectrometer with positive polarity, and detecting the positrons. The probability to produce neutral pions is large at larger scattering angles, and increases with decreasing scattered electron energy. For the E03-103 data at 40 (50)degrees, the charge symmetric back ground was $\approx 20\%$ (50%) for heavy nuclei at small x values.
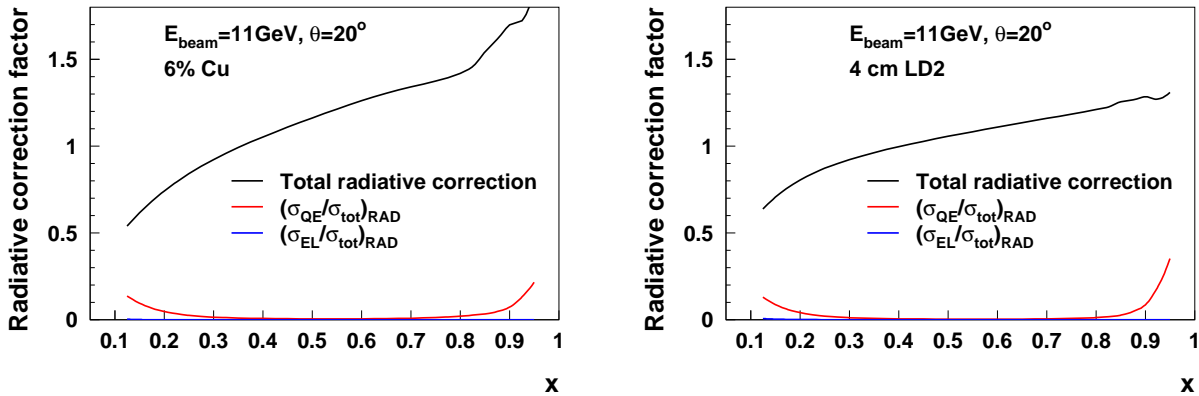

FIG. 11: Radiative correction factors estimated for the Cu (left) and ^{2}H targets for 20 degrees. Different contributions to the radiated cross sections are also shown. Here, red curve represents the relative contribution from quasi-elastic and the blue curve represents the relative contribution from elastic tail to the radiated cross sections.

Figure 10 shows the estimated charge symmetric back ground (using a model developed by P. Bosted, shown to be consistent with the E03–103 data) as a a function x for the 35 degree data. This figure shows the ratio of positron cross section to the sum of positron and electron cross sections. For the proposed measurements, the charge symmetric background will be the greatest for the thickest targets at the lowest x values. The background is much smaller for the lighter targets, and drops rapidly as one increases x or decreases the scattering angle. We plan to make direct measurements of the charge symmetric backgrounds at the lowest x values where the CSBG was found to be significant.

Similarly, radiative corrections (primarily the contribution of low-Q^2 quasielastic events radiating into the low x bins) become large for the lowest x values at small scattering angles. Figure 11 shows the estimated radiative correction factors for the 20 degree data for Cu (6% radiation length) and ^{2}H targets. Relative contributions from various radiative processes

Activity	Time (hours)
Production Running (incl. dummy)	406
Kinematic changes	24
Checkout/calibration	24
Target Boiling Studies	16
Hydrogen elastics	16
Positron runs	24
BCM calibrations	8
Target changeover	24
Radiative corrections check	8
Total	23 days

TABLE II: Approximate beam time required for the proposed experiment. The time shown is for SHMS and HMS taking data simultaneously.

such as the elastic and quasielastic processes to the radiated cross sections are also shown in the same figure. We note that the contributions from the quasielastic and nuclear elastic radiative tails are relatively small, even at the lowest x, and, based on the extensive studies done for the E03-103 measurement, we are confident that we can apply these corrections reliably for the angles where measurements are proposed.

An additional correction that needs to be applied to the data is due to the acceleration of the incoming electrons and deceleration of outgoing electrons in the Coulomb field of the target nucleus (so called Coulomb corrections). These correction factors are estimated using an improved version of the Effective Momentum Approximation (EMA) as described in [41]. For the proposed measurements Coulomb correction factors are found to be less than a percent for all light nuclei.

Based on the experience with the E03-103 analysis, we believe that we can adequately treat and account for all the corrections mentioned above.

D. Beam time request

Table II is a summary of the estimated beam time required for the measurement. Run times have been estimated assuming 0.5% statistics in each x bin for $W^2 > 3$ and at least 1% statistics for $3 > W^2 > 2$ for each target (0.5% for deuterium, which generally has a shorter run time). Note that for the ^{7}Li running at the highest x and largest Q^2, we will take about half the typical statistics due to the need to run at low currents. We request 23 days in Hall C in order to carry out the measurements described in this proposal.

Source	Absolute Uncertainty	Relative Uncertainty	$\delta\sigma/\sigma(\%)$	$\delta R/R(\%)$ point-to-point	$\delta R/R(\%)$ scale	$\delta R/R$ (%) Statistical
Spectrometer momentum	<0.1%	0.01%	0.2	-	-	
Beam Energy	<0.1%	<0.02%	0.2	-	-	
θ	0.5mr	0.2mr	0.5–1	0.4	-	
Beam angle	0.5mr	0.1mr	0.1	-	-	
t_D	1%		1	-	0.5	
t_A	0.5–1.0%		0.5–1.0	-	0.5–1.6	
Charge	0.4%	0.2%	0.5	0.2	0.2	
Target Boiling	<0.5%	0.2%	<0.5	0.1	0.2–0.4	
End-cap Subtraction	<1.0%	0.2%	<1.0	0.1	0.1	
Acceptance	1.0-2.0%	0.2%	1.0-2.0	0.3	0.5	
Radiative Corrections	2.0%	0.5%	2.0	0.2–0.4	0.4	
Detector Efficiency	0.5%	0.2%	0.5	0.2	-	
Deadtime Correction	<0.5%	0.2%	<0.5	0.1	0.2	
Positron Background	0.2%	0.2%	0.2	0.1–0.3	0.2	
Total			2.93–3.62	0.64–0.78	1.04–1.9	0.7–1.2

TABLE III: Estimated systematic uncertainties in the ratio $\sigma_A/\sigma_{^2H}$. For $x < 0.9$, the statistical uncertainties will be 0.7–1.2%. The point–to–point systematic error in the target ratios will be 0.6–0.8% and the overall systematic error will range from 1–1.9%, depending on the target.

E.   Estimated systematic uncertainties and projected results

Target	Radiation length (%)	Uncertainty in thickness (%)
^{6,7}Li	0.4	1.0
^{10,11}B	1.2	0.5
Be	2	0.5
C	1.5	0.5
^{40,48}Ca	4	1.0
Cu	6	1.0

TABLE IV: Proposed solid targets for the experiment and the estimated uncertainty in thicknesses. Larger uncertainty in calcium and lithium targets are partially due to the difficulty in handling those targets.

We estimate a systematic uncertainty of $\approx 3.3\%$ in the absolute cross sections for most of the kinematics. To correct for density changes due to localized heating in the deuterium target, we will measure rate as a function of current. Many sources of uncertainty will cancel in the cross section ratios for different targets, and we estimate a final point–to–point

Target	Target length (cm)	Uncertainty in thickness (%)
^{1,2}H	4	0.8
^{3}He	4	1.6
^{4}He	4	1.2

TABLE V: Proposed cryo targets for the experiment and the estimated uncertainty in thicknesses.

systematic uncertainty in the ratios of approximately 0.7% and an overall scale systematic uncertainty of 1–1.5%. Table III shows the contributions to the systematic uncertainties in the target ratios. The solid targets will be measured at the same time as the deuterium target, and so will not have uncertainties in the EMC ratios due to uncertainties in the kinematics. However, they will have some uncertainty in the acceptance, due to the difference in the target length. Note that the uncertainty in the thickness of the deuterium target is a common uncertainty for the σ_A/σ_{2H} ratios for all targets. Table V and IV shows the contributions to the systematic uncertainties due to the uncertainty in thickness measurement of the targets.
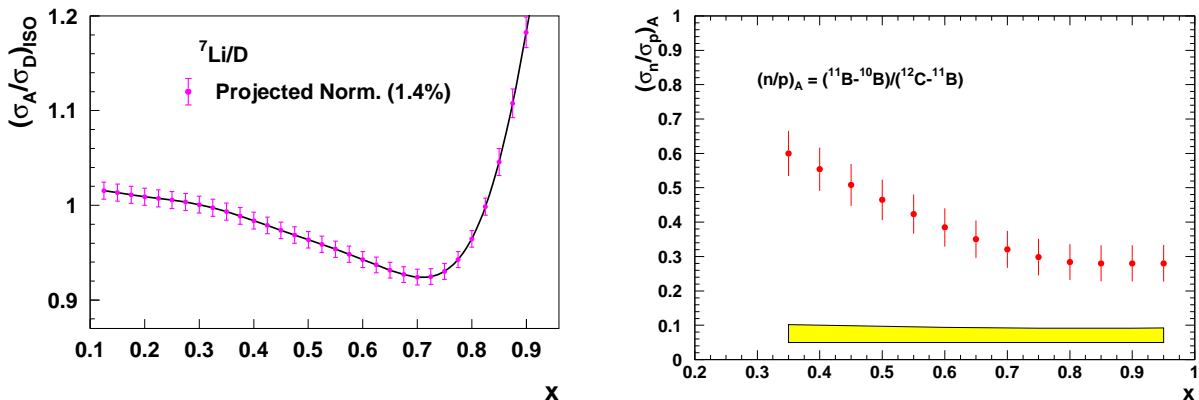

FIG. 12: The plot on the left panel shows the projected uncertainties for the ^{7}Li EMC ratios. Error bars indicate statistical and point-to-point systematic uncertainties combined in quadrature, while global, scale, uncertainties are indicated separately. The black line shown is the SLAC parametrization for the x dependence of the EMC effect. The plot on the right side shows projected uncertainties in the in-medium n/p ratio extracted from ^{11}B and ^{10}B and ^{12}C.

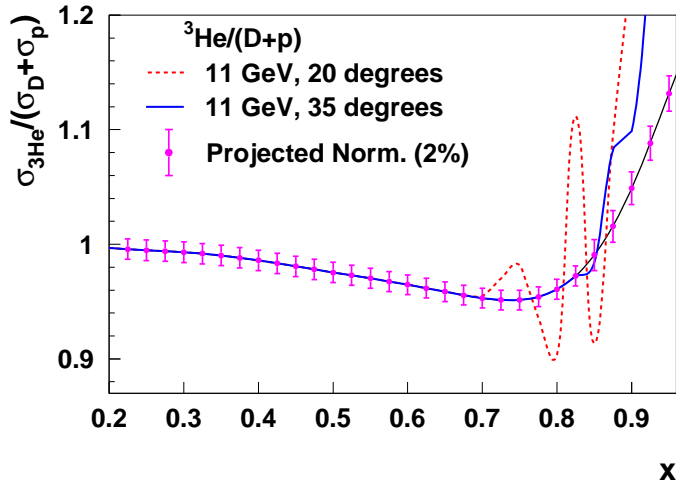Figure 12 and figure 13 shows the projected uncertainties for some of the proposed measurements.

FIG. 13: The figure shows the projected uncertainties for the ^{3}He/(^{2}H+^{1}H) ratios. The red dotted line shows the ratios (using a model) for the 20 degree kinematic setting while the solid blue line shows the same ratios at 35 degrees. Note that the structure in the ratios (due to the resonance contribution) is pushed to higher x values as one increases the scattering angle.

V.   EXPERIMENTS WITH SIMILAR PHYSICS GOALS

This experiment is an extension of the 6 GeV EMC effect measurement, as discussed in detail in the proposal. There is a completed experiment, E03-104, still under analysis, aimed at extracting the form factor ratio G_{Ep}/G_{Mp} for a proton in ^{4}He, which is also meant to probe nuclear modification to proton structure. As discussed in the introduction, that experiment is technically more challenging and is sensitive to final state interactions, but the results, if they can be cleanly interpreted, directly connect to the question of whether or not the internal structure of the nucleon is modified in the nucleus. As such, the two experiments are extremely complementary.

VI.   SUMMARY

We request 23 days in Hall C to measure inclusive scattering from hydrogen, deuterium, ^{3}He, ^{4}He, ^{6,7}Li, ^{9}Be, ^{10,11}B, ^{12}C, ^{40,48}Ca, and ^{63}Cu for $0.1 < x < 1$. We will take data on deuterium and C to examine the Q^2-dependence of the nuclear structure functions and the EMC ratio. This measurement will be in the traditional DIS region up to x=0.8, and beyond that it takes advantage of the precise extended scaling seen in nuclear structure functions and target ratios. We will measure the EMC effect with high precision at large x, and we will do precise measurements of the x dependence in the low x region.

The high x measurements on light nuclei will provide strict constraints on calculations of EMC effect which must include binding and nuclear wave-function effects. Since the conventional nuclear effects lead to modifications of the structure functions at all x values, a quantitative understanding is important before the addition of more exotic effects which may be required to explain the detailed nuclear dependence. In addition, the non-trivial A-dependence observed in light nuclei can be better studied with the addition of high precision measurements on additional light nuclei. The proposed measurements will provide a single data set with the EMC ratios for a range of light and medium heavy nuclei thus providing a comprehensive, precise basis to test state of the art models that attempt to explain the observed nuclear dependence.

---

[1] J. J. Aubert et al., Phys. Lett. B **123**, 123 (1983).

[2] D. F. Geesaman, K. Saito, and A. W. Thomas, Ann. Rev. Nucl. Part. Sci. **45**, 337 (1995).

[3] P. R. Norton, Rept. Prog. Phys. **66**, 1253 (2003).

[4] M. Arneodo, Phys. Rep. **240**, 301 (1994).

[5] S. Strauch et al. (Jefferson Lab E93-049), Phys. Rev. Lett. **91**, 052301 (2003).

[6] I. C. Cloet, W. Bentz, and A. W. Thomas, Phys. Rev. Lett. **95**, 052302 (2005).

[7] D.-H. Lu, K. Tsushima, A. W. Thomas, A. G. Williams, and K. Saito, Phys. Rev. **C60**, 068201 (1999).

[8] R. Schiavilla, O. Benhar, A. Kievsky, L. E. Marcucci, and M. Viviani, Phys. Rev. Lett. **94**, 072303 (2005).

[9] J. R. Smith and G. A. Miller, Phys. Rev. **C70**, 065205 (2004).

[10] J. R. Smith and G. A. Miller, Phys. Rev. **C72**, 022203 (2005).

[11] J. R. Smith and G. A. Miller, Phys. Rev. **C65**, 055206 (2002).

[12] J. R. Smith and G. A. Miller, Phys. Rev. Lett. **91**, 212301 (2003).

[13] E. Marco, E. Oset, and P. Fernandez de Cordoba, Nucl. Phys. **A611**, 484 (1996).

[14] E. Marco and E. Oset, Nucl. Phys. **A645**, 303 (1999).

[15] D. M. Alde et al., Phys. Rev. Lett. **64**, 2479 (1990).

[16] J. J. Aubert et al., Nucl. Phys. B **293**, 740 (1987).

[17] A. C. Benvenuti et al., Phys. Lett. B **189**, 483 (1987).

[18] J. Gomez et al., Phys. Rev. D **49**, 4348 (1994).

[19] M. Arneodo et al. (New Muon.), Nucl. Phys. **B441**, 12 (1995).

[20] P. Amaudruz et al. (New Muon), Nucl. Phys. **B441**, 3 (1995).

[21] J. Seely et al., Phys. Rev. Lett. **103**, 202301 (2009).

[22] B. W. Filippone et al., Phys. Rev. C **45**, 1582 (1992).

[23] J. Arrington et al., Phys. Rev. C **64**, 014602 (2001).

[24] J. Arrington, R. Ent, C. E. Keppel, J. Mammei, and I. Niculescu, Phys. Rev. C **73**, 035205 (2006).

[25] L. L. Frankfurt, M. I. Strikman, D. B. Day, and M. Sargsian, Phys. Rev. **C48**, 2451 (1993).

[26] K. S. Egiyan et al. (CLAS), Phys. Rev. C **68**, 014313 (2003).

[27] K. S. Egiyan et al. (CLAS), Phys. Rev. Lett. **96**, 082501 (2006).

[28] R. Subedi et al., Science **320**, 1476 (2008).

[29] G. I. Smirnov, Eur. Phys. J. **C10**, 239 (1999).

[30] O. Benhar, private communication.

[31] S. C. Pieper and R. B. Wiringa, Ann. Rev. Nucl. Part. Sci. **51**, 53 (2001).

[32] K. Saito, K. Tsushima, and A. W. Thomas, Prog. Part. Nucl. Phys. **58**, 1 (2007).

[33] I. C. Cloet, W. Bentz, and A. W. Thomas, Phys. Lett. **B642**, 210 (2006).

[34] P. Solvignon, D. Gaskell, and J. Arrington, AIP Conf. Proc. **1160**, 155 (2009), arXiv:0906.0512.

[35] J. Arrington, F. Coester, R. J. Holt, and T. S. H. Lee, J. Phys. **G36**, 025005 (2009).

[36] A. Accardi et al. (2009), arXiv:0911.2254.

[37] M. Hirai, S. Kumano, and T.-H. Nagai, Phys. Rev. **C76** (2007).

[38] L. W. Whitlow, E. M. Riordan, S. Dasu, S. Rock, and A. Bodek, Phys. Lett. **B282**, 475 (1992).

[39] W. Melnitchouk and A. W. Thomas, Phys. Lett. **B377**, 11 (1996).

[40] J. Arrington, P. Solvignon, D. Higinbotham, and D. B. Day, spokespersons, Jefferson lab experiment E08-014.

[41] A. Aste, C. von Arx, and D. Trautmann, Eur. Phys. J. **A 26**, 167 (2005).

New Measurements of the European Muon Collaboration Effect in Very Light Nuclei

J. Seely,[1] A. Daniel,[2] D. Gaskell,[3] J. Arrington,[4,*] N. Fomin,[5] P. Solvignon,[4] R. Asaturyan,[6,†] F. Benmokhtar,[7] W. Boeglin,[8]
B. Boillat,[9] P. Bosted,[3] A. Bruell,[3] M. H. S. Bukhari,[2] M. E. Christy,[10] B. Clasie,[1] S. Connell,[5,‡] M. M. Dalton,[5] D. Day,[5]
J. Dunne,[11] D. Dutta,[11,12] L. El Fassi,[4] R. Ent,[3] H. Fenker,[3] B. W. Filippone,[13] H. Gao,[1,12] C. Hill,[5] R. J. Holt,[4] T. Horn,[7,3]
E. Hungerford,[2] M. K. Jones,[3] J. Jourdan,[9] N. Kalantarians,[2] C. E. Keppel,[10] D. Kiselev,[9] M. Kotulla,[9] C. Lee,[14]
A. F. Lung,[3] S. Malace,[10] D. G. Meekins,[3] T. Mertens,[9] H. Mkrtchyan,[6] T. Navasardyan,[6] G. Niculescu,[15] I. Niculescu,[15]
H. Nomura,[16] Y. Okayasu,[2,16] A. K. Opper,[17] C. Perdrisat,[18] D. H. Potterveld,[4] V. Punjabi,[19] X. Qian,[12] P. E. Reimer,[4]
J. Roche,[3] V. M. Rodriguez,[2] O. Rondon,[5] E. Schulte,[4] E. Segbefia,[10] K. Slifer,[5] G. R. Smith,[3] V. Tadevosyan,[6] S. Tajima,[5]
L. Tang,[10] G. Testa,[9] R. Trojer,[9] V. Tvaskis,[10] W. F. Vulcan,[3] F. R. Wesselmann,[5] S. A. Wood,[3] J. Wright,[5]
L. Yuan,[10] and X. Zheng[4]

[1]*Laboratory for Nuclear Science, Massachusetts Institute of Technology, Cambridge, Massachusetts, USA*
[2]*University of Houston, Houston, Texas, USA*
[3]*Thomas Jefferson National Laboratory, Newport News, Virginia, USA*
[4]*Physics Division, Argonne National Laboratory, Argonne, Illinois, USA*
[5]*University of Virginia, Charlottesville, Virginia, USA*
[6]*Yerevan Physics Institute, Yerevan, Armenia*
[7]*University of Maryland, College Park, Maryland, USA*
[8]*Florida International University, Miami, Florida, USA*
[9]*Basel University, Basel, Switzerland*
[10]*Hampton University, Hampton, Virginia, USA*
[11]*Mississippi State University, Jackson, Mississippi, USA*
[12]*Triangle Universities Nuclear Laboratory, Duke University, Durham, North Carolina, USA*
[13]*Kellogg Radiation Laboratory, California Institute of Technology, Pasadena, California, USA*
[14]*University of the Witwatersrand, Johannesburg, South Africa*
[15]*James Madison University, Harrisonburg, Virginia, USA*
[16]*Tohoku University, Sendai, Japan*
[17]*Ohio University, Athens, Ohio, USA*
[18]*College of William and Mary, Williamsburg, Virginia, USA*
[19]*Norfolk State University, Norfolk, Virginia, USA*

New Jefferson Lab data are presented on the nuclear dependence of the inclusive cross section from ^{2}H, ^{3}He, ^{4}He, ^{9}Be and ^{12}C for $0.3 < x < 0.9$, $Q^2 \approx 3$–6 GeV^2. These data represent the first measurement of the EMC effect for ^{3}He at large x and a significant improvement for ^{4}He. The data do not support previous A-dependent or density-dependent fits to the EMC effect and suggest that the nuclear dependence of the quark distributions may depend on the *local* nuclear environment.

High energy lepton scattering provides a clean method of probing the quark momentum distributions in nucleons and nuclei. The early expectation was that probes at the GeV energy scale would be insensitive to nuclear binding effects, which are typically on the order of several MeV. The effects were expected to be small except at large Björken-x, corresponding to very high momentum quarks. In this region, the rapid falloff of the parton distributions approaching the kinematical limit of $x \to 1$ makes the distributions very sensitive to the smearing effect of the nucleon's motion.

In 1983 the European Muon Collaboration (EMC) discovered that the per-nucleon deep inelastic structure function, $F_2(x)$, in iron was significantly different than that for deuterium [1]. They showed a clear suppression of high momentum quarks for $0.3 < x < 0.8$, confirmed for several

nuclei in more extensive measurements at SLAC [2]. This phenomenon, dubbed the ''EMC effect,'' has become the subject of a determined theoretical effort aimed at understanding the underlying physics. While progress has been made in explaining the principal features of the effect, no single model has been able to explain the effect over all x and A [3,4]. Much of the effort has focused on heavy nuclei, and many models are evaluated for infinite nuclear matter and scaled to the density of finite nuclei, neglecting possible surface effects or the impact of detailed nuclear structure.

There has been less focus on few-body nuclei, which provide the opportunity to test models in cases where the details of the nuclear structure are well understood. These data are also necessary to get a complete picture of the evolution of nuclei from deuterium to infinite nuclear

matter. Precise measurements in few-body nuclei allow for stringent tests of calculations of the effects of Fermi motion and nuclear binding, which is the dominant effect at large x. In addition, these data allow us to test simple scaling models of the EMC effect. A global analysis of the SLAC data [2] found that the data could be equally well described by fits that assumed the EMC effect to be proportional to the average nuclear density, ρ, or by fits that assumed it scaled with the nuclear mass, i.e., an EMC effect proportional to $\ln(A)$. These simple fits for the nuclear dependence did equally well for heavy nuclei ($A \gtrsim 12$), where the density varies slowly with A. For very light nuclei, these simple models predict different behavior, but the limited data on light nuclei were not sufficient to differentiate between these predictions.

To address these issues, Jefferson Lab (JLab) experiment E03-103 was proposed to make high precision measurements of the EMC effect at large x in both heavy and few-body nuclei. The experiment ran in Hall C during the fall of 2004. The measurement used a 5.767 GeV, 80 μA unpolarized electron beam, with scattered electrons detected in the High Momentum Spectrometer (HMS). The primary measurements were taken at a scattering angle of 40°, with additional data taken at different angles and/or 5 GeV beam energy to examine the Q^2 dependence. Data were collected on four cryotargets—^{1}H, ^{2}H, ^{3}He, and ^{4}He, and solid Beryllium, Carbon, Copper, and Gold targets arranged together on a common target ladder. The target ladder held only two cryotargets at a time, so there were two separate running periods to collect data on all four cryogenic targets. Data were taken on solid targets during both periods for systematic checks on the relative normalization during the two run periods. In this Letter, we focus on the light nuclei, $A \leq 12$, for which fewer data exist and which require smaller corrections due to backgrounds and Coulomb distortion.

The HMS subtends a solid angle of 7 msr and the momentum bite was restricted to the central part of the acceptance ($\pm 9\%$). The detector package consisted of two sets of wire chambers for tracking, four planes of hodoscopes for triggering, and a gas Čerenkov and lead-glass calorimeter for online and offline particle identification [5]. The cross sections were corrected for electronic and computer dead times, detector efficiencies, and radiative effects (which closely followed the approach of Ref. [6]). Data were taken at several beam currents on carbon to look for rate-dependent corrections, and on all four cryotargets to measure current-dependent target density effects due to heating at high current.

The dominant sources of background were pion production, electrons scattering from the aluminum cryocell wall and electrons from pair-production in the target. After applying calorimeter and Čerenkov cuts, the pion contamination was negligible for the kinematics shown here. The electron background (8%–19%) from the cell wall was subtracted using measurements on a "dummy" target, consisting of two aluminum targets at the positions of the cryocell walls, with radiative corrections calculated separately for the real cryocells and the dummy target. The background from pair production was measured by reversing the HMS polarity to detect positrons, yielding a direct measure of the charge-symmetric background, strongly dominated by pair production. This background was typically 5%–10%, but was as much as 30% of the total yield at the lowest x and largest Q^2 values.

There are several sources of systematic uncertainty which we separate into point-to-point and normalization uncertainties. Normalization uncertainties are those that modify the overall scale, but not the x or Q^2 dependence of the target cross section ratios, e.g., target thicknesses. Point-to-point uncertainties can vary with x or Q^2, and are treated in the same way as statistical uncertainties.

The cryogenic target thicknesses were determined from the dimensions of the cryocell and the density of the cryogen, as computed from measurements of its pressure and temperature. The total normalization uncertainty in the cross section ratios was between 1.6% and 1.9%, mainly due to the 1%–1.5% uncertainty in the target thicknesses. Uncertainty in the target boiling correction contributes ~0.4%, radiative corrections [6] contribute 0.1%–0.75%, depending on the kinematics and target thickness, and the acceptance contributes 0.5% (0.2%) to the solid target (cryotarget) ratios. The dominant sources of point-to-point uncertainties come from charge measurement drifts (0.3%), corrections due to drift of beam position on target (0.45%), radiative corrections (0.5%), dead time determination (0.3%), detector efficiencies (0.3%), and acceptance (0.3%). Charge-symmetric background subtraction contributes 0.1%–0.6% to the uncertainty, and is largest for the Be and C targets. The uncertainties in the kinematics contribute up to 0.6% to the uncertainties in the ratios, with larger effects at large x values where the cross section is changing most rapidly. We apply Coulomb distortion corrections following the effective momentum approximation of Aste [7]. The corrections are $\lesssim 1\%$ for ^{12}C, and much smaller for the helium data.

The results are shown as ratios of the cross section per nucleon, rather than the F_2 structure functions. These ratios are identical if the ratio of longitudinal to transverse cross sections, $R = \sigma_L/\sigma_T$, is independent of A. If $R_A \neq R_D$, then there will be a correction involved in going from cross section ratios to the F_2 ratios [3].

In the Björken limit, the structure function exhibits scaling, i.e., becomes independent of Q^2 except for the weak Q^2 dependence from QCD evolution of the parton distributions. This scaling has been observed in the deep-inelastic scattering region, which for e-p scattering is typically taken to be $Q^2 > 1$ GeV^2 and $W^2 > 4$ GeV^2, where W is the invariant mass of the unmeasured system. In nuclei, it has been observed that results are nearly

independent of Q^2 to lower values of W^2 for $Q^2 \gtrsim 3$ GeV^2 [8]. A precise measurement of the target ratios in the resonance region [9] for $Q^2 = 3$–4 GeV^2 showed that the nuclear dependence is identical to the high Q^2 measurements up to $x \approx 0.8$, even though the deep-inelastic scattering region is limited to $x < 0.5$ for these Q^2 values.

Because these data are at somewhat lower Q^2 than previous high-x results, typically $Q^2 = 5$ or 10 GeV^2 for SLAC E139 [2], extensive measurements were made to verify that our result is independent of Q^2. The structure functions were extracted at several Q^2 values and found to be consistent with scaling violations expected from QCD down to $Q^2 \approx 3$ GeV^2 for $W^2 \geq 1.5$ GeV^2, while the structure functions ratios show no Q^2 dependence. Figure 1 shows the carbon to deuteron ratio for the five highest Q^2 settings (the lowest and middle Q^2 values were measured with a 5 GeV beam energy). There is no systematic Q^2 dependence in the EMC ratios, even at the largest x values, consistent with the observation of previous measurements [3].

For all further results, we show the ratios obtained from the 40° data (filled squares in Fig. 1). While there are data at 50° (open circles) for all nuclei, the statistical precision is noticeably worse, and there are much larger corrections for charge-symmetric background and Coulomb distortion (for heavier nuclei).

The EMC ratios for ^{12}C, ^{9}Be, and ^{4}He are shown in Fig. 2 along with results from previous SLAC extractions. The ^{4}He and ^{12}C results are in good agreement with the SLAC results, with much better precision for ^{4}He in the new results. While the agreement for ^{9}Be does not appear to be as good, the two data sets are in excellent agreement if we use the same isoscalar correction as E139 (see below) and take into account the normalization uncertainties in the two data sets. In all cases, the new data extend to higher x, although at lower W^2 values than the SLAC ratios. The

EMC ratio for ^{4}He is comparable to ^{12}C, suggesting that the modification is dependent on the average nuclear density, which is similar for ^{4}He and ^{12}C, rather than a function of nuclear mass.

Figure 3 shows the EMC ratio for ^{3}He, with the low-x data from HERMES. Note that the HERMES ^{3}He data have been renormalized by a factor of 1.009 based on comparisons of their ^{14}N EMC effect and the New Muon Collaboration ^{12}C result [10]. We show both the measured cross section ratio (squares) and the "isoscalar" ratio (circles), where the ^{3}He result is corrected for the proton excess. Previous high-x EMC measurements used a correction based on an extraction of the F_{2n}/F_{2p} ratio for free nucleons from high Q^2 measurements of F_{2d}/F_{2p}. We use global fits [11,12] to the free proton and neutron cross sections evaluated at the kinematics of our measurement and then broadened using the convolution procedure of
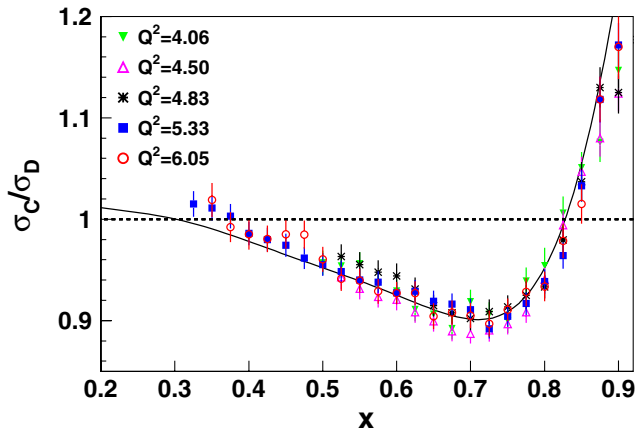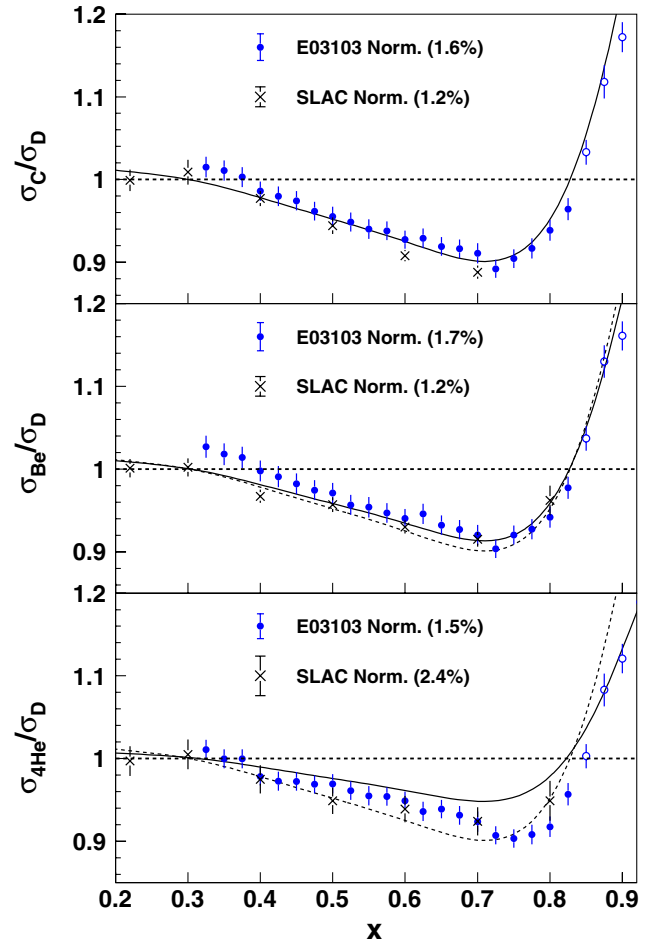

FIG. 1 (color online).   Carbon EMC ratios [17] for the five highest Q^2 settings (Q^2 quoted at $x = 0.75$). Uncertainties are the combined statistical and point-to-point systematic. The solid curve is the SLAC fit [2] to the Carbon EMC ratio.

FIG. 2 (color online).   EMC ratios for ^{12}C, ^{9}Be, and ^{4}He [17], compared to SLAC [2]. The ^{9}Be results include a correction for the neutron excess (see text). Closed (open) circles denote W^2 above (below) 2 GeV^2. The solid curve is the A-dependent fit to the SLAC data, while the dashed curve is the fit to ^{12}C. Normalization uncertainties are shown in parentheses for both measurements.
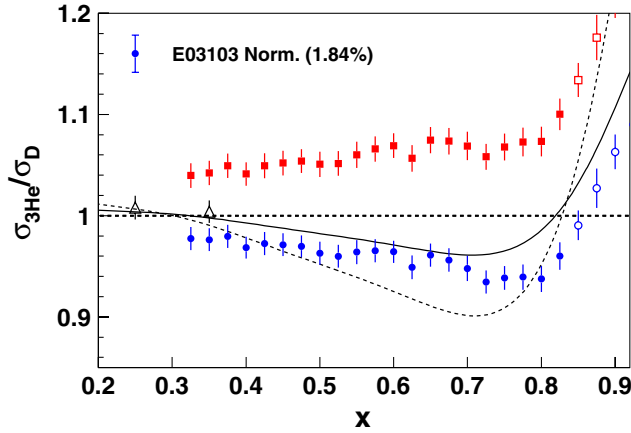
FIG. 3 (color online). EMC ratio for ^{3}He [17]. The upper squares are the raw ^{3}He/^{2}H ratios, while the bottom circles show the isoscalar EMC ratio (see text). The triangles are the HERMES results [10] which use a different isoscalar correction. The solid (dashed) curves are the SLAC A-dependent fits to carbon and ^{3}He.

Ref. [13] to yield the neutron-to-proton cross section ratio in nuclei. Using the "smeared" proton and neutron cross section ratios more accurately reflects the correction that should be applied to the nuclear ratios, and in the end, yields a significantly smaller correction at large x, where the uncertainty in the neutron structure function is largest.

While applying the isoscalar correction to the ^{3}He data using the smeared F_{2n}/F_{2p} ratio yields a more reliable result, there is still some model dependence to this correction due to the uncertainty in our knowledge of the neutron structure function. Ref. [13] demonstrated that much of the inconsistency between different extractions of the neutron structure function comes from comparing fixed-Q^2 calculation to data with varying Q^2 values, rather than from the underlying assumptions of nuclear effects in the deuteron. Nuclear effects beyond what is included in Ref. [13], such as the off-shell contribution $\delta^{(\text{off})}$ of Ref. [14], yield a 1%–2% decrease to the proton's contribution to the deuteron thus increasing the extracted F_{2n}/F_{2p} ratio by 0.01–0.02. This yields a slightly reduced correction for ^{3}He which would raise the isoscalar EMC ratio for ^{3}He by 0.3%–0.6% at our kinematics.

The observed nuclear effects are clearly smaller for ^{3}He than for ^{4}He and ^{12}C. This is again consistent with models where the EMC effect scales with the average density, as the average density for ^{3}He is roughly half that of the ^{12}C. However, the results of ^{9}Be are not consistent with the simple density-dependent fits. The observed EMC effect in ^{3}He is essentially identical to what is seen in ^{12}C, even though the density of ^{9}Be is much lower. This suggests that both the simple mass- or density-scaling models break down for light nuclei.

One can examine the nuclear dependence based on the size of the EMC ratio at a fixed x value, but the normal-

ization uncertainties become a significant limiting factor. If we assume that the shape of the EMC effect is universal, and only the magnitude varies with target nucleus, we can compare light nuclei by taking the x dependence of the ratio in the linear region, $0.35 < x < 0.7$, using the slope as a measure of the relative size of the EMC effect that is largely unaffected by the normalization. The slopes are shown for light nuclei in Fig. 4 as a function of average nuclear density. The average density is calculated from the *ab initio* Greens Function Monte Carlo calculation of the spatial distributions [15]. Because we expect that it is the presence of the other $(A - 1)$ nucleons that yields the modification to the nuclear structure function, we choose to scale down this density by a factor of $(A - 1)/A$, to remove the struck nucleon's contribution to the average density. The EMC effect for ^{3}He is roughly one third of the effect in ^{4}He, in contrast to the A-dependent fit to the SLAC data [2], while the large EMC effect in ^{9}Be contradicts a simple density-dependent effect.

One explanation for the anomalous behavior of ^{9}Be is that it can be described as a pair of tightly bound alpha particles plus one additional neutron [16]. While most of the nucleons are in a dense environment, similar to ^{4}He, the *average* density is much lower, as the alphas (and additional neutron) "orbit" in a larger volume. This suggests that it is the *local* density that drives the modification. The strong clustering of nucleons in ^{9}Be leads to a special case where the average density does not reflect the local environment of the bulk of the protons and neutrons.

Another possibility is that the x dependence of the EMC effect is different enough in these light nuclei that we cannot use the falloff with x as an exact measure of the relative size of the EMC effect. This too suggests that the EMC effect is sensitive to the details of the nuclear structure, which would require further theoretical examination. At the moment, there are almost no calculations for light nuclei that include detailed nuclear structure.
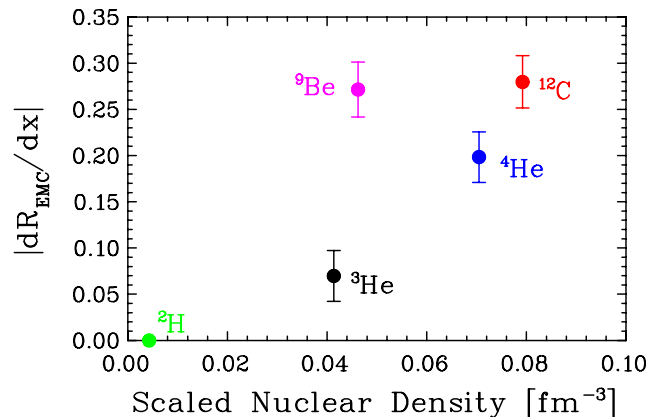

FIG. 4 (color online). The circles show the slope of the isoscalar EMC ratio for $0.35 < x < 0.7$ as a function of nuclear density. Error bars include statistical and systematic uncertainties.

In conclusion, we have measured the nuclear dependence of the structure functions for a series of light nuclei. This data set provides significantly improved data on ^{4}He and the first valence-region measurement on ^{3}He, as well as extending the measurements to higher x for other light nuclei. This will allow for more detailed comparison with calculations that include binding and Fermi motion, providing a more reliable baseline at low x, where these effects are still important, but may not fully explain the observed nuclear dependence.

These data also provide model independent information on the scaling of the nuclear effects. Under the assumption that the shape of the EMC effect is the same for all nuclei, the large difference between ^{3}He and ^{4}He rules out previous A-dependent fits, while the EMC effect in ^{9}Be is inconsistent with models where the effect scales with average density. The results are consistent with the idea that the effect scales with the *local* environment of the nucleons, or require that the x dependence of the effect changes in very light nuclei.

---

*Corresponding author: johna@anl.gov
†Deceased

‡Present address: University of Johannesburg, Johannesburg, South Africa.

[1] J. Aubert *et al.*, Phys. Lett. B **123**, 275 (1983).
[2] J. Gomez *et al.*, Phys. Rev. D **49**, 4348 (1994).
[3] D. F. Geesaman, K. Saito, and A. W. Thomas, Annu. Rev. Nucl. Part. Sci. **45**, 337 (1995).
[4] P. R. Norton, Rep. Prog. Phys. **66**, 1253 (2003).
[5] D. Dutta *et al.*, Phys. Rev. C **68**, 064603 (2003).
[6] S. Dasu *et al.*, Phys. Rev. D **49**, 5641 (1994).
[7] A. Aste, C. von Arx, and D. Trautmann, Eur. Phys. J. A **26**, 167 (2005).
[8] J. Arrington *et al.*, Phys. Rev. C **64**, 014602 (2001).
[9] J. Arrington, R. Ent, C. E. Keppel, J. Mammei, and I. Niculescu, Phys. Rev. C **73**, 035205 (2006).
[10] K. Ackerstaff *et al.* (HERMES), Phys. Lett. B **475**, 386 (2000); **567**, 339(E) (2003).
[11] M. E. Christy and P. E. Bosted arXiv:0712.3731.
[12] P. E. Bosted and M. E. Christy, Phys. Rev. C **77**, 065206 (2008).
[13] J. Arrington, F. Coester, R. J. Holt, and T. S. H. Lee, J. Phys. G **36**, 025005 (2009).
[14] W. Melnitchouk, A. W. Schreiber, and A. W. Thomas, Phys. Lett. B **335**, 11 (1994).
[15] S. C. Pieper and R. B. Wiringa, Annu. Rev. Nucl. Part. Sci. **51**, 53 (2001).
[16] K. Arai, Y. Ogawa, Y. Suzuki, and K. Varga, Phys. Rev. C **54**, 132 (1996).
[17] See EPAPS Document No. E-PRLTAO-103-015948 for data tables and figures. They are also available for download at http://hallcweb.jlab.org/experiments/E03103. For more information on EPAPS, see http://www.aip.org/pubservs/epaps.html.